# Optical Fiber Probe Transit Anemometer for Particle Velocity Measurements in Fluidized Beds

A compact optical fiber probe to measure the velocity of solid particles in two-phase flows was constructed. The probe has been used to measure particle velocities and obtain flow trajectories of solids in the distributor grid region of a two-dimensional fluidized bed. Air was used as the fluidizing medium in a bed of glass beads of size ranging from 0.2 to 0.7 mm.

Particle velocities were measured at corresponding points within a jet in the two-dimensional bed, using the optical fiber probe and a Laser Doppler Velocimeter (LDV). The probe measurements compare well with the LDV results in the main jet region. Particle velocities were also measured with the probe in the dense phase region of the fluidized bed where measurements were not possible using LDV. The resulting flow maps clearly indicate solids circulation patterns around jets and identify dead zones formed on the distributor plate.

**B. PATROSE and**
**H. S. CARAM**
Department of Chemical Engineering
Lehigh University
Bethlehem, PA 18015

## SCOPE

Intense mixing between bed solids and the entering gas occurs in the grid region of a fluidized bed. Quantitative information on solid motion in this region is required for a better design of a distributor plate appropriate for a given operation.

The objective of the present work is to measure solid particle velocities in the grid region and identify the effects of operating parameters on solids circulation and dead zone formation in this region. Methods available for two-phase flow measurement employ indirect techniques to obtain particle velocities, and often require probes that are large and disturb the flow.

Perturbations to the flow can be avoided if optical techniques are used. They include the well known high-speed photography and the relatively new laser velocimetry. The main difficulty is, however, that they require an optical path to the measurement volume that is not available in the opaque three-dimensional beds. Nevertheless, in the few configurations where such a path exists they provide a good technique for the evaluation and calibration of other probes. In this study a fine optical fiber probe was used to measure particle velocities in a two-dimensional fluidized bed using transit time correlation.

## CONCLUSIONS AND SIGNIFICANCE

The possibility of measuring solid velocity in the neighborhood of the distributor plate has been demonstrated. The measurements also show that the assumption of two-dimensional behavior in flat beds is valid except in the immediate neighborhood of the grid orifices, since no velocity differences were found across the thickness of the bed. Velocities measured using the optical fiber probe are presented in flow maps (Figures 8–10) that indicate solids circulation patterns and stagnant regions formed near the distributor plate.

The transit time correlation approach using the optical fiber probe was found to be a convenient technique to measure particle velocities in two-phase flows with minimal interference to the flow. The technique is easy to apply and does not require prior knowledge of the flow orientation. It also does not require alignment or orientation along the direction of flow as one would when using a pitot tube. Two transit time measurements made 90 degrees apart are sufficient to determine the magnitude and direction of the particle velocity.

---

## INTRODUCTION

The proper design of the distributor has been identified as the key to the successful operation of a fluidized bed reactor (Wen and Dutta, 1977). Many investigators have indicated that gas and solid contacting is more efficient near the grid than higher up in the bed. Further, the distributor design greatly influences the physical and chemical performance of the bed (Bottom, 1970; Behie and Kehoe, 1973; Cooke et al., 1968).

Much qualitative information can be found on the importance and nature of gas and solids mixing in the grid region. However, very little quantitative information has been reported to adequately describe the flow characteristics of gas and solids in the region close to the grid plate.

A schematic representation of possible gas and solids flow patterns near the grid region is shown in Figure 1. It is our objective to study the effects of operating variables on the structure of the jet, the solid circulation patterns and dead zone formation in this region. The design and application of the optical fiber transit anemometer for particle velocity measurement is described. The optical fiber probe was used to measure particle velocities in a two-dimensional fluidized bed using the transit time correlation technique. The probe is small in size and its insertion into a flow would result in minimal interference. The use of the probe does not require apriori knowledge of the flow orientation, nor does it

Correspondence concerning this paper should be addressed to H. S. Caram.
0001-1541-82-5516-0604-$2.00 

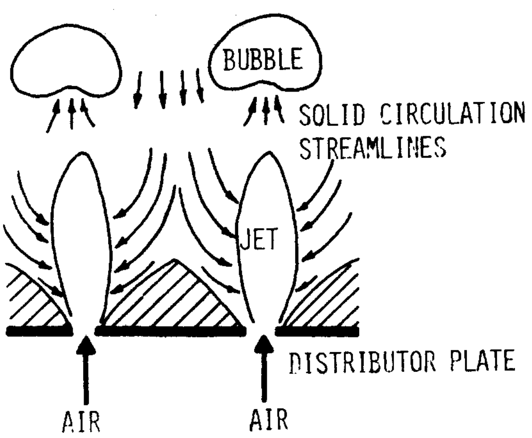


**Figure 1. Schematic representation of solids flow pattern and dead zone formation in the grid region, After Wen and Dutta (1977).**

require alignment or orientation along the direction of flow. However, the probe requires calibration and a dual beam LDV was used as the standard for calibration.

Techniques available for two-phase flow measurement are those based on impact, thermal, electrical and optical methods.

In the impact strain gage (Heertjes et al., 1970; Livshits and Tamarin, 1979) one measures the solids momentum. To calculate the solids flow it is necessary to simultaneously determine the bed porosity. They have been used, however, in conjunction with high-speed photography to measure local solids concentration (Donadono et al., 1980; Donsi et al., 1980). Thermal techniques were used by Marsheck and Gomezplata (1965) to measure the local mass flow rate by relating it to the rate of heat transfer between two closely located thermistors. The probe had to be aligned with the flow and calibrated for different types of bed material. Electrical methods using resistance or capacitance measurements have been used in pneumatic transport systems by measuring the transit time of the naturally occurring noise at two positions along the axis of the conveyor (Beck et al., 1968; Beck et al., 1973).

Visual techniques available include high-speed photography which is useful in dilute systems (Donadono et al., 1980; Donsi et al., 1980; Donadono and Massimilla, 1978; Knowlton and Hirsan, 1980), analysis of the traces of periodically excited fluorescent particles (Yong et al., 1980), and follow up of tracer particles (Latif and Richardson, 1972). These methods are precise and non-intrusive but the large number of measurements required for a statistically significant result makes them very tedious.

Laser Doppler Velocimetry can be used when an optical path is available to the measurement site (Birchenough and Mason, 1976; Lee and Srinivasan, 1977; Morton and Clark, 1971). It has the advantage of requiring no calibration. In cases where an optical path to the point of measurement is unavailable, the light transmission ability and small size of optical fibers have been used to develop optical fiber probes using the transit time method (Hemstrom et al., 1976; Miller and Mitchie, 1969; Oki et al., 1977). Such a probe was used by Shirai et al. (1977) to measure particle velocities in the neighborhood of a disk rotating in a bed of particles and of a bubble rising in a fluidized bed.

The measurements in the present work were performed using an optical fiber probe with light being transmitted through the central fibers and reflected light from the particles being received through two other fibers. The time delay, $\tau_o$, between the signals collected by the two receiving fibers was used to compute the velocity knowing the distance $l_{AB}$ between fibers:

$$U_p = l_{AB}/\tau_o$$

and it is found from the location of the maximum of the cross correlation function

$$\Phi_{AB}(\tau) = \frac{1}{T}\int_0^T A(t)\,B(t+\tau)\,dt \tag{1}$$

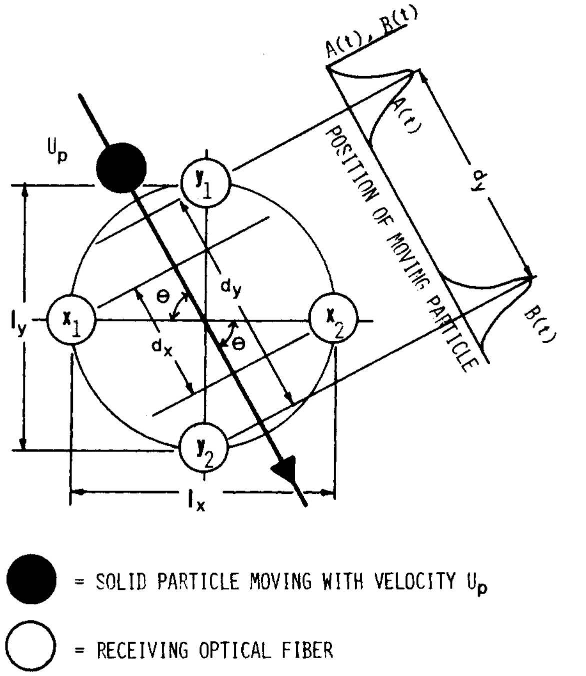


**Figure 2. Schematic of the measuring system.**

with $T \gg \tau_{max}$. A discussion of this approach is presented in Kiphan (1978).

## EXPERIMENTAL

### Probe Construction and Measurement Technique

A compact optical fiber probe was constructed for this study using five illuminating fibers to achieve a uniform and intense illumination of the region of the flow field where the measurement is made. The fibers were encased in a hypodermic needle for mechanical strength and rigidity. The individual fibers were 0.125 mm in diameter and the probe outer diameter was 0.85 mm. The probe was 30 mm in length and could be introduced into the 2-D bed to various penetrations across the bed thickness. To ensure good light transmission through the probe, the fiber tips were polished using 1 $\mu$m alumina on a felt polishing wheel.

Figure 2 represents a head-on view of the probe where the thick solid line represents the trajectory of a particle moving with velocity $U_p$ at an angle $\theta$ to the horizontal. Also shown are the relative variations in intensity of the reflected light captured by the receiving fibers at locations $y_1$ and $y_2$. They show a maximum in the reflected light intensity as the particle passes closest to the corresponding fiber. The time delay $\tau_y$ between the two maxima is the time taken for the particle moving at velocity $U_p$ to traverse a distance $d_y$. Therefore,

$$U_p = \frac{d_y}{\tau_y} = \frac{d_x}{\tau_x}$$

where the same analysis has been applied to the signals collected by the fibers located at $x_1$ and $x_2$, and delayed by time $\tau_x$.

In practice, $\tau_x$ and $\tau_y$ are the transient times computed by the correlator using the cross-correlation technique. The magnitude $|U_p|$ and direction ($\theta$) of the flow are determined using the relations

$$U_p = \left[\left(\frac{\tau_y}{l_y}\right)^2 + \left(\frac{\tau_x}{l_x}\right)^2\right]^{-1/2} \tag{2}$$

and

$$\theta = \arctan\left[\frac{\tau_y}{\tau_x}\cdot\frac{l_x}{l_y}\right] \tag{3}$$

Equations 2 and 3 specify the magnitude of the particle velocity and its direction, and thereby completely define the projection of the particle velocity vector on the plane perpendicular to the tip of the fiber probe.

Notice that since the sign of the time delay is known from the cross-correlation function, it becomes possible to determine the orientation of the flow, and the directional ambiguity encountered in Laser Doppler Velocimetry is eliminated.

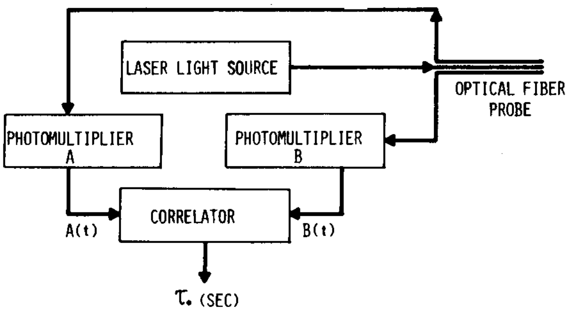


**Figure 3. Instrumentation and signal flow diagram.**

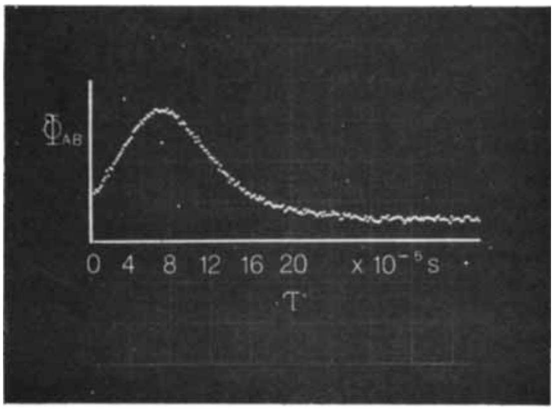


**Figure 4. A typical cross-correlation function computed by the correlator.**

$$\Phi_{AB}(\tau) = \frac{1}{T}\int_0^T A(t)\,B(t+\tau)\,dt$$

### Fluidized Bed Apparatus

The particle velocity measurements were carried out in a 305 × 19 mm rectangular cross-sectional bed with transparent Plexiglas walls. The nozzles in the distributor plate were of 19 × 3.2 mm rectangular cross section, spaced 50 mm apart, and had porous packing in them to produce a uniform distribution of air through the nozzles. Glass beads were used as the bed material (particle density = 2,470 kg/m$^3$, mean diameter = 500 $\mu$m, standard deviation from the mean = 86.2 $\mu$m). The air used was humidified by bubbling through a tank of water, which significantly reduced the buildup of static charge on the glass beads and bed walls. At the bed entrance the air was at 21°C with relative humidity varying between 60 and 100%.

The probe was introduced through a 64 × 50 mm test grid composed of an array of 0.9 mm holes spaced 2.5 mm apart. The grid extended 64 mm above from the top level of the distributor.

Local average particle velocities were measured in this study. Since the receiving fibers are positioned a very short distance apart, a typical particle transit time between these fibers is very small (~$10^{-4}$ s) in comparison to the total sampling time of the correlator (~$10^2$ s). The computed velocity will therefore always be an average over the sampling time (though small). Ishida et al. (1980) have recently reported unsteady state particle velocity measurements using a multifiber optical probe in conjunction with a microcomputer data processor where the signals received by the optical fibers were recorded by an analog data recorder and subsequently processed to compute instantaneous velocities.

The instrumentation block diagram of the setup used in the present investigation is shown in Figure 3. The light source used was a 15 mW He-Ne

TABLE 1. EFFECTIVE DISTANCE COMPUTATION

| $y$ Location [mm] | LDV Measurement $U_p$ [m/s] | Transit Time $\tau_o$ [s] | Effective Distance $l = U_p \cdot \tau_o$ [m] |
|---|---|---|---|
| 20 | 0.75 | $1.95 \times 10^{-4}$ | $1.46 \times 10^{-4}$ |
| 40 | 0.91 | $1.45 \times 10^{-4}$ | $1.32 \times 10^{-4}$ |
| 60 | 1.04 | $1.25 \times 10^{-4}$ | $1.3 \times 10^{-4}$ |
| 100 | 1.56 | $0.95 \times 10^{-4}$ | $1.48 \times 10^{-4}$ |
| 200 | 2.33 | $0.65 \times 10^{-4}$ | $1.51 \times 10^{-4}$ |

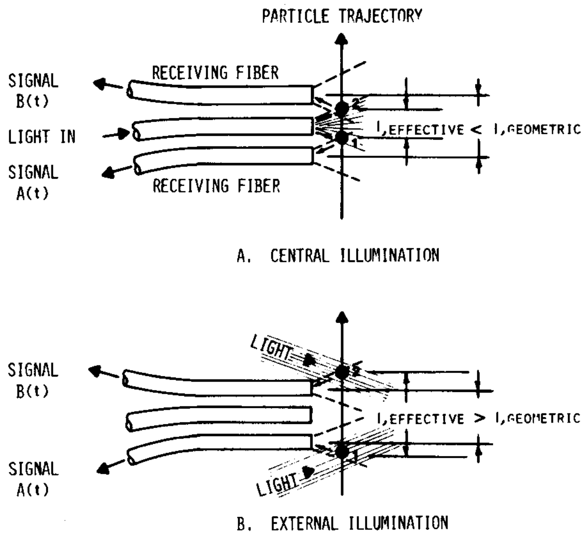


**Figure 5. Influence of illumination and fiber viewing angle on the effective distance. The shaded area indicates illumination and the dashed lines indicate the viewing angle of the receiving fibers.**

laser. The variations of reflected light, captured by the receiving fibers in the probe, were converted to electric signals $A(t)$ and $B(t)$ by photomultipliers. These signals were fed to the correlator (Honeywell SAI-43A, correlation and probability analyzer). The computed cross-correlation function given by Eq. 1 was displayed on an oscilloscope. The time delay $\tau_o$ was obtained by reading the location of the maximum of the displayed correlogram (Figure 4).

## RESULTS AND DISCUSSIONS

### Probe Calibration

The use of Eqs. 2 and 3 requires the knowledge of $l_x$ and $l_y$, the effective fiber to fiber separation distance. One would intuitively expect the value of $l$ to be used in these equations, to be equal to the actual center to center distance between the receiving fibers. To verify this calibration experiments were performed in a free-falling stream of glass beads ($d_p$ = 500 $\mu$m), and the value of $l$ was calculated from the particle velocity measurements made using dual beam Laser Doppler Velocimetry (LDV). Since LDV is an absolute technique, no calibration is required. The free jet configuration was chosen for calibration of the probe because it approximates very closely the two-phase nature of the bed in which the actual particle velocity measurements were made.

Particle velocity measurements were made using dual beam LDV at different locations within the falling stream of particles. At each location the probe was positioned such that its front tip exactly coincided with the measuring volume formed by the two Laser beams of the LDV. This ensured that the transit time information obtained from the probe corresponded to the particle velocity measured by the LDV. The particle velocity $U_p$ and the transient time $\tau_o$ were used to compute the effective fiber to fiber separation distance $l$. Table 1 includes a representative set of calibration data. The average effective distance $l$ was found to be 0.14 mm; whereas, the actual geometric center to center distance between the two receiving fibers was measured under the microscope to be 0.37 mm. The "apparent" or "effective" distance is seen to be a function of the viewing angle of the receiving fibers and the nature of illumination produced at the measuring site (Figure 5). Two extreme cases of illumination are discussed here.

Figure 5(A) represents the case where only one central fiber is used to illuminate the measuring site. The shaded area indicates the cone of illumination produced in the region immediately in front of the fiber. The dashed lines indicate the angle of vision of the receiving fibers which is a characteristic of the optical fiber. Light from beyond the angle of vision is not captured by the receiving fibers since the angle of incidence is smaller than that re-

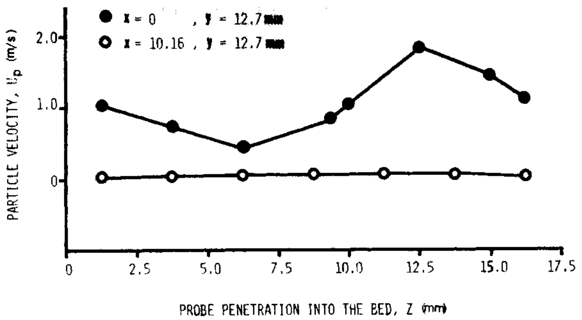


**Figure 6. Variation of particle velocity along the bed thickness. Verification of two-dimensional nature using the optical fiber probe.**

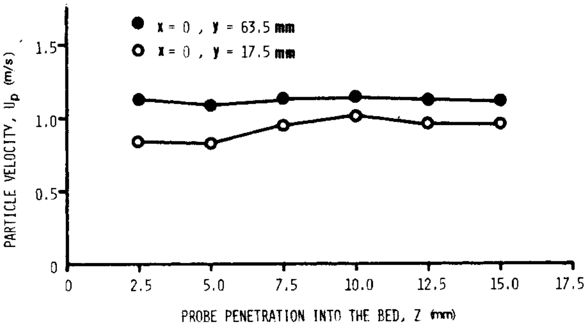


**Figure 7. Variation of particle velocity along the thickness of the jet. Verification of two-dimensional nature using the LDV.**

quired for total internal reflection to occur within the fiber. It can be seen that the bottom fiber receives maximum reflected light from the moving particle when the particle reaches position 1. Similarly, the top fiber receives maximum reflected light when the particle reaches position 2. Therefore, the delay between maxima will be smaller than that expected if the maximum intensity were to occur when the particle passed over the fiber center. The inverse effect is observed if no light is introduced through the central fiber, and the measuring site is illuminated from beyond the two receiving fibers. The effective distance computed for this case would therefore be greater than the geometric separation distance (Figure 5(B)). This was confirmed by experiments done with the same probe ($l_{geometric} = 0.37$ mm) and using two different types of illumination. External illumination gave a computed effective distance of 0.42 mm, and using internal illumination gave an effective distance of 0.14 mm.

If the measuring site is very uniformly illuminated, the computed effective distance would be expected to exactly equal the geometric fiber separation distance. This would also be the case if the viewing angle of the receiving fibers was equal to zero. These effects are currently being investigated using different optical fibers and configurations within the probe. It should, however, be noted that it is of little consequence whether the computed effective distance for a particular probe is equal to or different from its geometric fiber to fiber separation distance. The only requirement is that the probe be calibrated to compute its $l_{effective}$, and this value be used for $l$ when computing velocities using Eq. 2.

The effectiveness of the probe was found to be independent of the nature of the particle surface and shape of individual particles. This was confirmed by using the probe to measure the surface velocity of a disc rotating at a known speed. The surface roughness of the disc produced identical waveforms through both receiving fibers, with one waveform lagging the other by a time equal to the transit time between the two detection points.

### Measurements in the Two-Dimensional Bed

*Verification of Two-Dimensional Behavior of the Bed.* Particle velocities were measured for a fixed air flow rate at different probe penetrations into the thickness of the bed. If the bed had ideal two-dimensional flow characteristics, there would be no variation across the bed thickness.

Figure 6 compares velocities measured at the jet axis with measurements made in the emulsion phase at the same elevation from the distributor. Figure 7 compares velocities along the jet axis at two distances from the nozzle. Velocities measured at the jet axis show variation across the thickness of the bed—indicating nonuniform distribution of air flow through the distributor nozzle. In the emulsion phase, however, the velocity remains almost unchanged across the bed thickness (Table 3). The variations caused by the nonuniformity in air flow across the nozzle width therefore die down with increasing lateral distance from the jet axis and also with increasing vertical distance from the nozzle.

Based on the observed nonideal two-dimensional flow characteristics, all other particle velocity measurements were made on the half plane of the bed.

*Comparison of Probe with LDV Measurements.* Particle velocities were measured at corresponding locations within a jet in the two-dimensional bed using the optical fiber probe and a Laser Doppler Velocimeter (LDV) for identical bed and flow conditions. The transparent walls and the two-dimensional geometry of the bed made it possible to use the LDV to measure velocities within the jet. The probe measurements agree well with the LDV results in the main jet region, and are compared in Table 2. Such a comparison made in the actual flow itself demonstrated the suitability of the optical fiber probe for particle velocity measurements within fluidized beds. It therefore would be possible to measure particle velocities within a three-dimensional bed using an optical fiber probe, whereas LDV would not be applicable.

*Bed Fully Penetrated by a Single Jet: Spout Case.* The bed was filled with particles to a depth of 43.2 mm. A single jet was created using air flow to only the central nozzle. Keeping the air flow rate constant at $1.7 \times 10^{-3}$ m$^3$/s produced a steady jet that fully penetrated the bed. Particle velocities were measured at various points in the bed by inserting the probe through the test holes in the bed wall, after allowing the flow to reach steady state. Figure 8 is a particle flow map on which each arrow indicates the direction of the velocity vector computed at that location using the optical fiber probe. The arrows have been joined to indicate particle trajectories observed qualitatively through the transparent bed walls as solids move downward in the dense region of the bed, are entrained in the jet, and are conveyed vertically upward in the central core. No particle motion was observed in the shaded dead zones.

Based on the computed particle flow map, the fully penetrated

TABLE 2. COMPARISON OF PARTICLE VELOCITIES MEASURED USING LDV AND THE OPTICAL FIBER PROBE AT CORRESPONDING LOCATIONS IN THE TWO-DIMENSIONAL BED ($h_t$ = 43.2 mm; $G_o = 2 \times 10^{-3}$ m$^3$/s)

| Location in $y$ | Bed (mm) $x$ | $U_p$, LDV (m/s) | $U_p$, Probe (m/s) | % Difference |
|---|---|---|---|---|
| 25.4 | 2.54 | 0.54 | 0.56 | 3.7 |
| 40.64 | 15.24 | 0.58 | 0.51 | 12.0 |
| 38.1 | 0 | 1.15 | 1.16 | 0.9 |
| 50.8 | 0 | 1.15 | 1.16 | 0.9 |
| 63.5 | 0 | 1.15 | 1.16 | 0.9 |

TABLE 3. VARIATION OF PARTICLE VELOCITY ALONG THE BED THICKNESS IN THE EMULSION PHASE ($x$ = 10.16, $y$ = 12.7 mm)

| Probe Penetration $z$ (mm) | $U_p$, Probe (mm/s) | Flow Orientation $\theta$ (degree) |
|---|---|---|
| 1.27 | 39.3 | 40.6 |
| 3.81 | 42.7 | 42.6 |
| 6.35 | 52.8 | 33.1 |
| 8.89 | 53.3 | 36.0 |
| 11.43 | 54.5 | 34.3 |
| 13.97 | 50.7 | 36.5 |
| 16.51 | 43.4 | 38.9 |

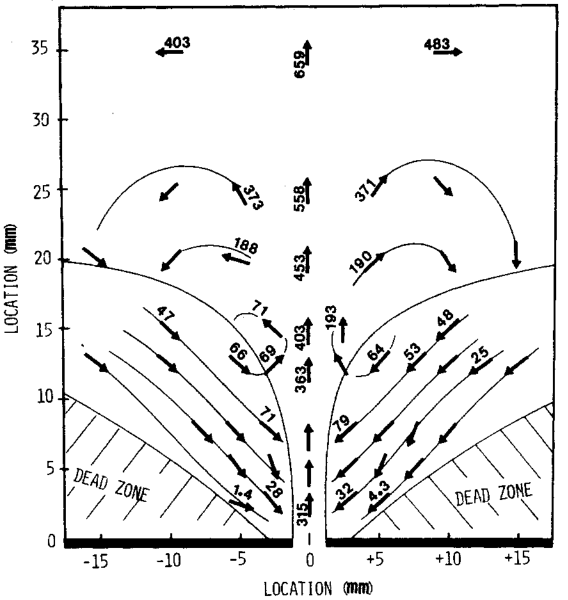


**Figure 8. Particle flow map of a spouted bed. Velocities indicated in mm/s (glass beads, $h_i$ = 43.2 mm, $G_o$ = 1.7 × $10^{-3}$ m³/s).**

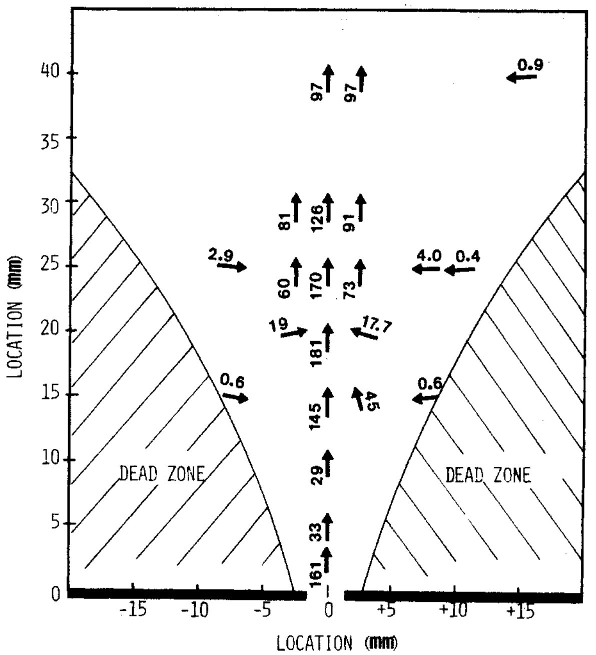


**Figure 9. Solids circulation above a gas inlet nozzle in a bed fluidized using five jets. Velocities indicated in mm/s (glass beads, $h_i$ = 184 mm, $G_o$ = 5.2 × $10^{-4}$ m³/s).**

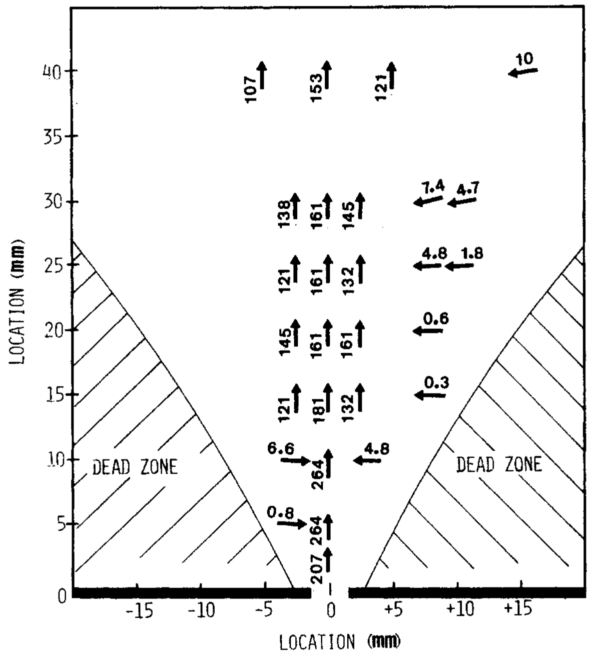


**Figure 10. Solids circulation above a gas inlet nozzle in a bed fluidized using five jets. Velocities indicated in mm/s (glass beads, $h_i$ = 184 mm, $G_o$ = 5.75 × $10^{-4}$ m³/s).**

bed may be viewed as composed of three rather distinct regions: a jet core, a narrow jet boundary region, and a packed bed region.

In the jet core region the solids entrained in the jet are pneumatically conveyed upward by the gas. The solid particles are accelerated upward initially and then may attain terminal velocity. Higher up in the 'spout' itself gas and particle velocities decrease and the particles return to the bed.

The major change in direction (downward to upward) of the particles is seen to occur in a very narrow jet boundary region. The particles in the packed bed region slide downward toward the jet nozzle and are entrained by the jet when they reach the jet boundary.

*Bed Fluidized Using Multiple Jets.* Initial bed height was 184 mm. The bed was fluidized using equal flow rates of air through each of the five nozzles on the distributor. Particle velocities were measured in the jet and in the region beyond the jet penetration lengths predicted by the correlations of Zenz (1968), Merry (1975), and Yang and Keairns (1978). Beyond the jet penetration length, the jet breaks down into a stream of fast-moving bubbles (Rowe et al., 1979).

Two different air flow rates were studied and the particle flow maps computed using the optical fiber probe are presented in Figures 9 and 10. The gas flow rate in case 1 (Figure 9) was 11.5% above minimum fluidization and the bed condition was observed to be smooth fluidization at the onset of bubbling. The gas flow rate in case 2 (Figure 10) was 25% above minimum fluidization and the bed was observed to be in the bubbling regime. Though the gas flow rate was only 10.6% higher than in case 1, the bubbling was considerably more pronounced in case 2 because of the transition from one fluidization regime to another.

Visual observation of the region above the gas inlet nozzle in case 1 clearly showed a short stem, about 6 mm long and 3 mm wide, whose top would close periodically and was followed by a chain of bubbles. Such a pinch point appears to indicate the height at which the entering gas jet chokes and cannot entrain additional solids. At that point the solids concentration is high and it corresponds to the bottom of a bubble beginning to rise. The particle velocity in this region was confirmed to be small from the probe measurements (Figure 9). In the higher gas velocity case, the "pinch point" cannot be located from the probe measurements in Figure 10 and may lie beyond the test grid.

It has not been possible to compare the particle velocity measurements done here with those reported by Donadono and Massimilla (1978) since this study was performed in a deeper bed using a multiple nozzle arrangement and at much lower nozzle velocities (~5 m/s vs. 90 m/s). Their work was done with a single jet fully penetrating a particle bed that was well fluidized using a porous plate distributor. Studies at higher gas velocities and using different distributor configurations are in progress.

## ACKNOWLEDGMENT

The assistance and encouragement of Drs. Yong Kim and Raymond Emrich is gratefully acknowledged. Support for this work was provided by the U.S. Department of Energy through contract ET-78-6-01-3383.

## NOTATION

$A(t)$ = signal transmitted by the fiber at point $A$
$B(t)$ = signal transmitted by the fiber at point B
$d_p$ = particle diameter
$d_x$ = component of $l_x$ in the flow direction
$d_y$ = component of $l_y$ in the flow direction
$G_o$ = inlet gas flow rate
$h_i$ = initial bed height
$l_{AB}$ = linear distance between points $A$ and $B$
$l_x$ = $x$ fiber separation distance
$l_y$ = $y$ fiber separation distance
$t$ = time
$T$ = sampling time
$U_p$ = particle velocity
$x$ = lateral distance from the jet axis
$y$ = axial distance from the nozzle
$z$ = probe penetration into the bed thickness

### Greek Letters

$\tau_o$ = transit time
$\Phi_{AB}$ = cross-correlation function
$\theta$ = flow orientation with respect to horizontal

## LITERATURE CITED


Beck, M. S., J. Drane, A. Plaskowski, and N. Wainwright, "Particle Velocity and Mass Flow Measurements in Pneumatic Conveyors," *Powder Tech.*, **2**, 269 (1968).

Beck, M. S., K. T. Lee, and N. G. Stanley-wood, "A New Method for Evaluating the Size of Solid Particles Flowing in a Turbulent Fluid," *Powder Tech.*, **8**, 85 (1973).

Behie, L. A. and P. Kehoe, "The Grid Region in a Fluidized Bed Reactor," *AIChE J.*, **19**, 1070 (1973).

Bottom, R. J., "Gas Solid Contacting in Fluidized Beds," *Chem. Eng. Prog. Symp. Ser.*, No. 101, **66**, 8 (1970).

Birchenough, A. and J. S. Mason, "Laser Anemometry Measurements in a Gas Solid Suspension Flow," *Optics and Laser Tech.*, **8**, 6, 253 (1976).

Cooke, M. J., W. Harris, J. Highley, and D. F. Williams, "Kinetics of Oxygen Consumption in Fluidized Bed Carbonizers," Tripartite Chem. Eng. Conf. Symp. on Fluidization I, p. 14, Montreal (1968).

Donadono, S., A. Maresca, and L. Massimilla, "Gas Injection in Shallow Beds of Fluidized Coarse Solids," *Ing. Chim. Ital.*, **16**, 1–2, 1 (1980).

——— and L. Massimilla, "Mechanics of Momentum and Heat Transfer Between Gas Jets and Fluidized Beds," *Fluidization*, Cambridge University Press, p. 375 (1978).

Donsi, G., L. Massimilla, and L. Colantuoni, "The Dispersion of Axi-Symmetric Gas Jets in Fluidized Beds," *Fluidization*, Plenum Press, New York, p. 295 (1980).

Heertjes, P. M., J. Verloop, and R. Willems, "The Measurement of Local Mass Flow Rates and Particle Velocities in Fluid-Solid Flows," *Powder Tech.*, **4**, 38 (1970).

Hemstrom, G., K. Moller, and B. Norman, "Boundary Layer Studies in Pulp Suspension Flow," **59**, 8, 115 (1976).

Ishida, M., T. Shirai, and A. Nishiwaki, "Measurement of the Velocity and Direction of Flow of Solid Particles in a Fluidized Bed," *Powder Tech.*, **27**, 1 (1980).

Kipphan, H. and F. Mesch, "Flow Measurement Systems Using Transit Time Correlation," *Flow Measurement of Fluids*, 409 (1978).

Knowlton, T. M. and I. Hirsan, "The Effect of Pressure on Jet Penetration in Semi-Cylindrical Gas Fluidized Beds," *Fluidization*, Plenum Press, New York, p. 315 (1980).

Latif, B. A. F. and J. F. Richardson, "Circulation Patterns and Velocity Distributions for Particles in a Liquid Fluidized Bed," *Chem. Eng. Sci.*, **27**, 1933 (1972).

Lee, S. L. and J. Srinivasan, "LDA Technique Applied to Two-Phase Flow," Two-Phase Flow Instrumentation Review Group Meeting, ONRR/NRC Proceedings, p. I. 4-1 (1977).

Livshits, Y. E. and A. I. Tamarin, "Solid-Phase Velocity Patterns in Free and Constrained Fluidized Beds," *J. Eng. Phy.*, **36**, 4, 418 (1979).

Marsheck, R. M. and A. Gomezplata, "Particle Flow Patterns in a Fluidized Bed," *AIChE J.*, **11**, 167 (1965).

Merry, J. M. D., "Penetration of Vertical Jets into Fluidized Beds," *AIChE J.*, **21**, 507 (1975).

Miller, N. and R. E. Mitchie, "The Development of a Universal Probe for Measurement of Local Voidage in Liquid-Gas Two-Phase Flow Systems," Eleventh National ASME/AIChE Heat Transfer Conf., p. 82, Minneapolis (1969).

Morton, J. B. and W. H. Clark, "Measurement of Two-Point Velocity Correlations in a Pipe Flow Using Laser Anemometers," *J. Phy. Ed. Sci. Instrum.*, **4**, 814 (1971).

Oki, K., P. Walawender, and L. T. Fan, "The Measurement of Local Velocity of Solid Particles," *Powder Tech.*, **18**, 171 (1977).

——— and T. Shirai, "Particle Velocity in Fluidized Bed," *Fluidization Tech. California Proceedings*, **I**, 95 (1975).

Rowe, P. N., H. J. MacGillvray, and D. J. Cheesman, "Gas Discharge from an Orifice into a Gas Fluidized Bed," *Trans. Instn. Chem. Engrs.*, **57**, 194 (1979).

Shirai, T., M. Ishida, Y. Ito, N. Inoue, and S. Kobayashi, "Rotation of a Horizontal Disc within an Aerated Particle Bed," *J. Chem. Eng. of Japan*, **10**, 1, 40 (1977).

Wen, C. Y. and S. Dutta, "Research Needs for the Analysis, Design, and Scaleup of Fluidized Beds," *AIChE Symp. Ser.*, No. 161, **73**, 1 (1977).

Yang, W. C. and D. L. Keairns, "Design and Operating Parameters for a Fluidized Bed Agglomerating Combustor/Gasifier," *Fluidization*, Cambridge University Press, Cambridge, p. 208 (1978).

Yong, J., Y. Zhiqing, Z. Li, and W. Zhanwen, "A Study of Particle Movement in a Gas Fluidized Bed," *Fluidization*, Plenum Press, New York, p. 365 (1980).

Zenz, F. A., "Bubble Formation and Grid Design," *Inst. Chem. Eng. Symp. Ser.*, No. 30, 136 (1968).


*Manuscript received March 30, 1981; revision received August 5, and accepted August 24, 1981*